Current Topics in Electrochemistry
Vol. 25, 2023

Review

Random processes in electroanalysis: organic particles in aqueous environments

Vera Žutić*
Rudjer Bošković Institute, Bijenička 54, 10 000 Zagreb, Croatia.

ABSTRACT

This review documents the re-emerged interest in traditional electroanalysis, amperometry at mercury drop electrodes, inspired by the discovery of stochastic adhesion signals of single soft particles at the dropping mercury electrode (DME), which preceded the development of single entity electrochemistry (SEE). The random occurrence of adhesion events is due to the spatial heterogeneity inherent to a dispersed system and to the stochastic nature of the particles' encounter with the electrode. The amperometric adhesion signals of individual microparticles contain unique information on their surfaces and the interfacial interactions that can be measured directly in the aqueous environment. These intrinsic properties are important for the biological activity and self-organization. The review covers studies in model dispersions of hydrocarbon droplets allowing the thermodynamics and dynamics of adhesion at the three-phase boundary to be defined. The new approach was extended to studies of adhesion signals from suspensions of living cells of marine algae to measure their surface charge density, organization and interfacial forces involved in adhesion. The extensive experimental research and modelling of single liposome adhesion signals, that followed, included some contradicting interpretations of the mechanism and kinetics of adhesion. Further research is clearly needed to critically evaluate interpretations of the stochastic adhesion signals at the molecular level. The combination of fast and direct particle characterization through their adhesion signals with high resolution imaging by atomic force microscopy (AFM) sets the observation window below the micrometer scale that allows direct characterization of submicron particle dynamics in marine environments by decoupling biotic production from abiotic self-assembly processes of biopolymers in their formation.

KEYWORDS: adhesion signals, amperometry, droplets, liposomes, living cells, marine vesicles, mercury drop electrode, stochastic events, thermodynamics of adhesion, three-phase boundary.

1. Introduction

This review presents a personal view on the early discovery of stochastic events at the dropping mercury electrode (DME) immersed in seawater, [1, 2] that inspired the extensive research in electroanalysis due to the unique possibility to characterize individual soft microparticles directly in their aqueous environment. These achievements preceded the more recent developments of single entity electrochemistry (SEE) [3 and references therein].

The phenomenon was discovered by accident, during measurement of surfactant activity, i.e. amount of surface active substances of a seawater sample by recording the polarographic maximum of oxygen reduction [4].

Streaming maxima on current vs. potential curves at DME have been reported in the polarographic literature as 'polarographic maxima' [4, 5] so that

*Email id: zutic@irb.hr

a large number of experimental observations is available. The maxima are induced by the instability inherent in electrochemical hydrodynamic systems - interfacial turbulence at the liquid-liquid interface. Frumkin [6] was the first to draw attention to the close relationship between the phenomena of polarographic maxima and the Marangoni effect [7]. Thus, stationary and nonstationary convective streamings are generated by surface tension gradients at the interface and amplified to macroscopic instabilities resulting in a measurable increase in current [8, 9]. Suppression of streaming maxima by surfactants provides a basis for their determination [4].

The apparent irregularity in recording polarograms in a fresh, untreated seawater sample could not be eliminated by electrical filtering of the signal, but only by filtering the seawater itself (passing it through the 0.45 μm pore filter). The perturbations on current-time curves of various amplitudes and frequency indicated a stochastic process, which was interpreted as random collision-coalescence events of single surface-active particles with the mercury electrode/seawater interface [10, 11]. A single perturbation, recorded on the amperometric current-time curve is schematically presented in Figure 1.

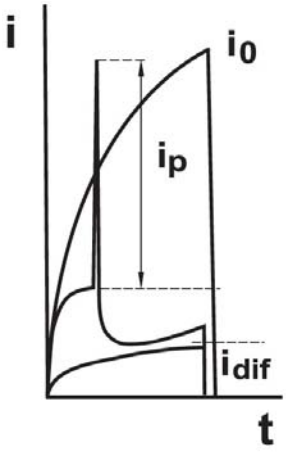

Figure 1. Schematic presentation of a single coalescence event on the current-time curve at the potential of polarographic maximum of oxygen reduction: i_0 is current in the absence of surfactants, i_{dif} is current at maximum suppression by surfactant adsorption, i_p is amplitude of the signal. The time scale is 2 seconds and current is in μA.

As such phenomenon has not been previously described in the literature, for its understanding it was necessary to develop theoretical concepts based on experiments with well-designed model systems. Two main research areas can be recognized:

1. Laboratory studies of attachment-spreading mechanism of organic droplets at the DME and the thermodynamics of adhesion at aqueous mercury electrode [10-18]. The stochastic adhesion signals of single soft particles, that were identified for the first time [10], were applied to characterize adhesion mechanisms and surfaces of individual living cells [17, 19-28] and liposmes [18, 29-38].
2. Field studies of vesicles' abundance and transformation in marine and estuarine environments [39-44] are leading to the emerging field of marine biophysics where emphasis is put on the organizational forces over chemical composition and to the processes on nano- and microscales to decouple biotic from abiotic processes in marine vesicles formation [45, 46]. A technical pilot experiment* demonstrated the possibility to record the stochastic adhesion signals directly in the sea with DME immersed in seawater. The air-saturated seawater is particularly suited for measurements of adhesion signals as a good electrolyte while the adhesion signals are amplified by the Faradaic charge transfer process of dissolved oxygen reduction.

2. Attachment-spreading of organic droplets at DME: thermodynamics and dynamics of adhesion

The mercury electrode surface is atomicaly smooth, fluid, and chemically inert, with well-known surface charge densities and interfacial tensions in a number of electrolyte solutions [47]. By varying the electrode potential from 0 to –1.5 V, the surface tension is precisely controlled in the range of 60 mJ/m^2 and surface charge density from +18 to -12 μC/cm. The reproducible formation of a

*Chevalet, J. and Hozić, A. 2002-2005, Žutić, V. Development of New Type of Electrochemical Sensor and Measurement System for Reactive Microparticles, Croatian Program for Innovative Technological Development (HITRA), Rudjer Bošković Institute, Zagreb, Croatia.

clean surface of DME is exploited for collection of a large set of data under identical experimental conditions since the arrival of particles to the electrode surface is a stochastic process [48, 49]. The representative behavior can be determined by analyzing a large set of time series collected under identical experimental conditions. The experimental method is the amperometric detection and analysis of stochastic electrical signals of single soft particles in an aqueous suspension by means of time-resolved data acquisition.

Wetting equilibrium [50, 51] and spreading in the three-phase system mercury (1), water (2), and organic liquid (3) could be predicted according to the modified Young-Dupré equation [16, 50, 51]. The total Gibbs energy of interaction between a hydrocarbon–droplet and the aqueous mercury interface is:

$$\Delta G = A(\gamma_{12} - \gamma_{13} - \gamma_{23}) \quad (1)$$

where γ_{12}, γ_{13} and γ_{23} are surface tensions at mercury/water, mercury/non-polar organic liquid and non-polar organic liquid/water interfaces, respectively.

The expression in parenthesis is equal to the spreading coefficient, the tendency of organic liquid (3) to spread onto interface

$$S_{132} = \gamma_{12} - \gamma_{13} - \gamma_{23} \quad (2)$$

For positive values of S_{132} the organic droplet will spread spontaneously and displace ions and water molecules from the interface (Figure 2.). For S_{132} <0 the spreading process will not proceed spontaneously [15].

If γ_{12} is independent of the applied potential, the spreading coefficient S_{132}, and thus the attachment and spreading of droplets is controlled by γ_{12}

$$\gamma_{12} = \gamma_{12}^{0} - \int_0^{E'} \sigma_{Hg}\, dE' \quad (3)$$

γ_{12}^{0} is surface tension at the potential of zero charge of the electrode, E_{pzc}, and $E' = E - E_{pzc}$.

Excellent agreement was obtained for critical interfacial tension of wetting, determined from critical potentials of attachment at DME [15-17] (Figures 3, 4) and the prediction based on the Good-Girifalco-Fowkes equation for the three-phase liquid system with hydrocarbon liquids C_{10}-C_{18}] [16, 18]. For the mercury/water/hexadecane system at the negatively charged DME the critical interfacial tension of wetting is 418.2 mJ/m^2 and at the positively charged DME it is 418.9 mJ/m^2, while 418.26 mJ/m^2 are the calculated values (Figure 3).

These experimental findings prove unambiguously that attachment and spreading of hydrocarbon droplets at the mercury electrode result in intimate contact between mercury and hydrocarbon, *i.e.*, adhesion in proper physicochemical sense.

The critical potentials of adhesion at DME, E_C^- and E_C^+, determined by polarography, (Figures 3, 4) represent well-defined and characteristic values for aqueous dispersions of organic liquids. The macroscopic properties of hydrocarbon liquids

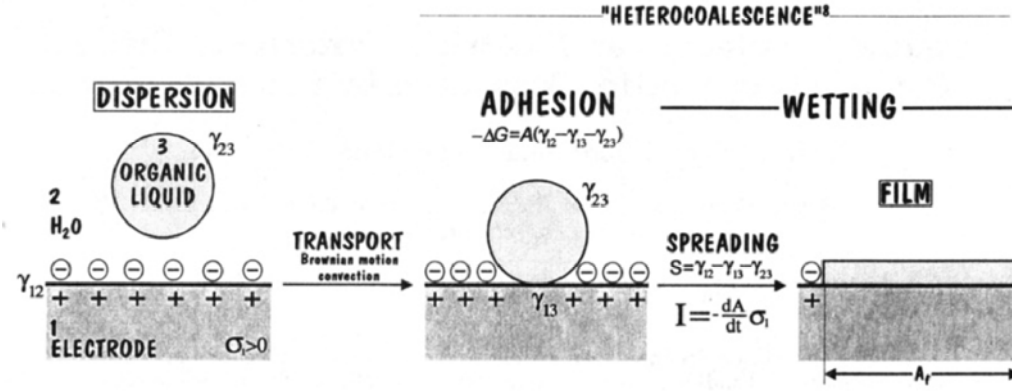

Figure 2. Schematic diagram of attractive interaction between dispersed organic droplets and a positively charged mercury electrode in an aqueous electrolyte solution. (Reprinted with permission from Ivošević, N., Tomaić, J. and Žutić, V. 1994, Langmuir, 10, 2415. Copyright (1994) American Chemical Society).

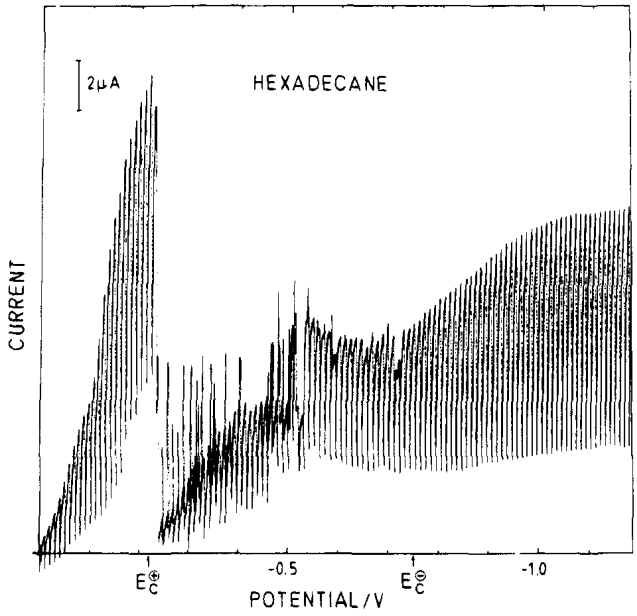

Figure 3. Polarogram of oxygen reduction in air-saturated dispersion of hexadecane: determination of critical potentials of attachment of hexadecane. E_c^+ and E_c^- are the predicted values. (E is electrode potential measured against Ag/AgCl reference) (Reprinted with permission from Ivošević, N., Tomaić, J. and Žutić, V. 1994, Langmuir, 10, 2415. Copyright (1994) American Chemical Society).

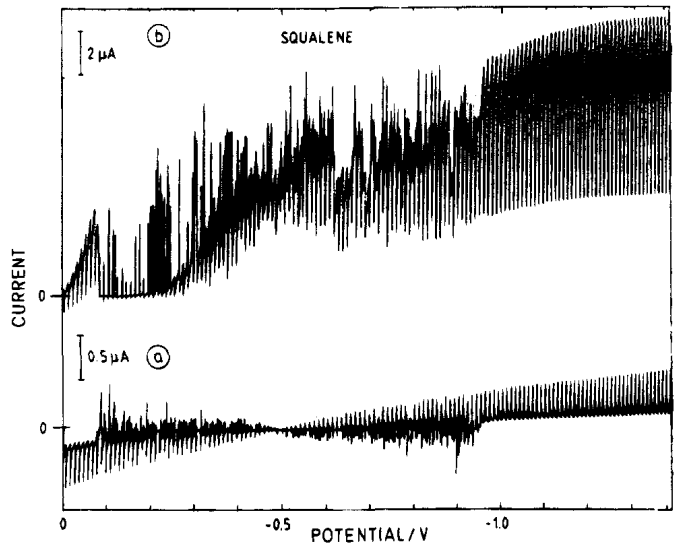

Figure 4. Charging current curve (a) and polarogram of oxygen reduction (b) in dispersion of squalene (180 mg L^{-1} in 0.1 M NaF) (Reprinted with permission from Ivošević, N., Tomaić, J. and Žutić, V. 1994, Langmuir, 10, 2415. Copyright (1994) American Chemical Society).

govern the interfacial interactions of microscopic droplets at the charged electrode/aqueous interface, offering predictions of interpolative nature for interactions of organic particles in the aquatic environment.

Adhesion and spreading of a soft organic particle

(droplet, cell, or liposome) at a charged mercury/ aqueous electrolyte interface cause double-layer charge displacement from the inner Helmholtz plane, and the transient flow of compensating current is recorded as an amperometric signal

$$I_D = -\frac{dA}{dt}\sigma_{12} \quad (4)$$

where I_D is the current caused by displacement of double-layer charge of the electrode, A_C is the area of the interacting interface of the electrode during particle adhesion, t is the time and σ_{12} is the surface charge density of the mercury/aqueous electrolyte interface.

Each amperometric signal corresponds to the adhesion of a single particle from suspension. The signal reflects the dynamics of the formation of adhesive contact and the subsequent rupture and spreading to a film of finite surface area. The rate of adhesion and spreading is enhanced by the hydrodynamic regime of the mercury electrode fluid interface [8, 17].

The random occurrence of the adhesion events is due to the spatial heterogeneity inherent to a dispersed system and to the stochastic nature of the particles' encounter with the electrode, whether it be a suspension of living cells [21] or suspension of liposomes [34]. These processes are stochastic in nature [48, 49] and are described by Poisson distribution.

At a given potential, the current amplitude reflects the size of adhered particle while the signal's frequency reflects the particles' concentration in the suspension. Signals are defined by their amplitude I_p, duration τ and the displaced charge q_D. The displaced double-layer charge, q_D, is obtained by integrating the area under the signal:

$$q_D = \int_{t_1}^{t_1+\tau} I_D\, dt \quad (5)$$

If charge displacement is complete, which leads to the formation of a monolayer, the area of the contact interface A_C is determined from the amount of displaced charge:

$$A_c = \frac{q_D}{\sigma_{12}} \quad (6)$$

where σ_{12} is the surface charge density of the mercury/aqueous electrolyte. The number of molecules in the monolayer is:

$$N = \frac{A_c}{A_M} \quad (7)$$

where A_M is the surface area per molecule.

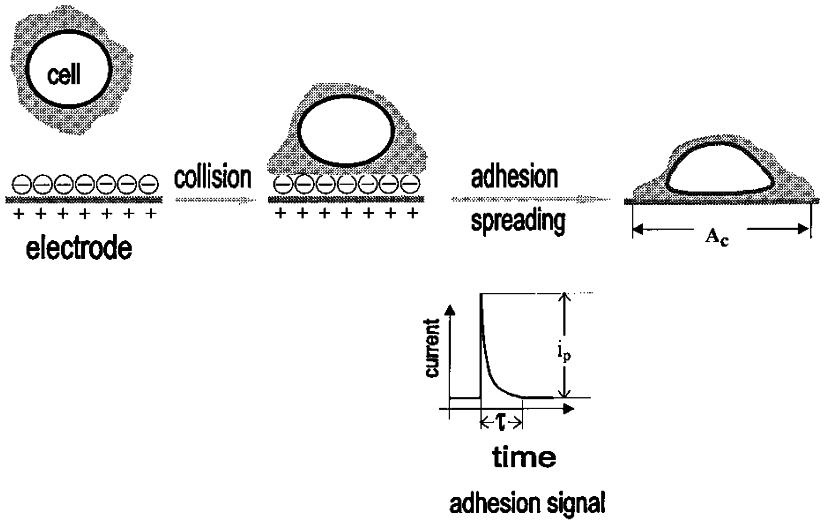

Figure 5. Schematic diagram of attractive interaction of a cell with a positively charged mercury electrode in an aqueous electrolyte solution. The current-time transient (adhesion signal) is caused by the double-layer charge displacement from the contact area A_C. (Reprinted with permission from Svetličić, V., Ivošević, N., Kovač, S. and Žutić, V. 2000, Langmuir, 16, 8217. Copyright (2000) American Chemical Society).

In the air-saturated systems the adhesion signals are amplified by the Faradaic charge transfer process of oxygen reduction, but could be further amplified by the addition of Hg(II) ions [10].

3. Adhesion signals of living cells

Cells with fluid or flexible outer membranes can readily form adhesive contact with the substrate [52] with little or no resistance to oppose deformation. Attractive interaction between a cell and mercury electrode results in the double-layer charge displacement, as illustrated in Figure 5. The flow of current (equation 4) is directly related to the formation of adhesion contact and subsequent spreading of a cell. The only hypothesis used in interpreting the experimental results is the validity of the classical double-layer model of charge distribution at electrode/solution interface [23], while the rate of adhesion and spreading of cells is enhanced by the hydrodynamic regime of the mercury electrode fluid interface [8, 17].

Unicellular marine algae, *D. tertiolecta* cells are suitable for electrochemical detection [20, 23] because of their size, membrane properties and euryhaline nature. The cells are simple to grow in the laboratory as axenic culture and in aqueous electrolyte solutions they form stable suspensions of single cells due to pronounced cell motility. The cells suspended in NaCl solutions can serve as a model system for studying cell surface interactions that could also be extended to mammalian cells.

The electrochemical response in a cell suspension is illustrated in Figure 6 by segments of current-time curves with the sequence of adhesion signals.

Each spike-shaped signal corresponds to the double-layer charge displacement by attachment of a single particle. Within the limiting potentials of appearance of signals, E_L^+ = -60 mV and E_L^- = -1300 (Figure 7) the net displacement current is in the same direction as the reduction current at the positively charged electrode, and the direction of current is reversed to the same direction as oxidation current at the negatively charged electrode. The signals are of a similar shape characterised by a steep rising portion followed by a slower decay

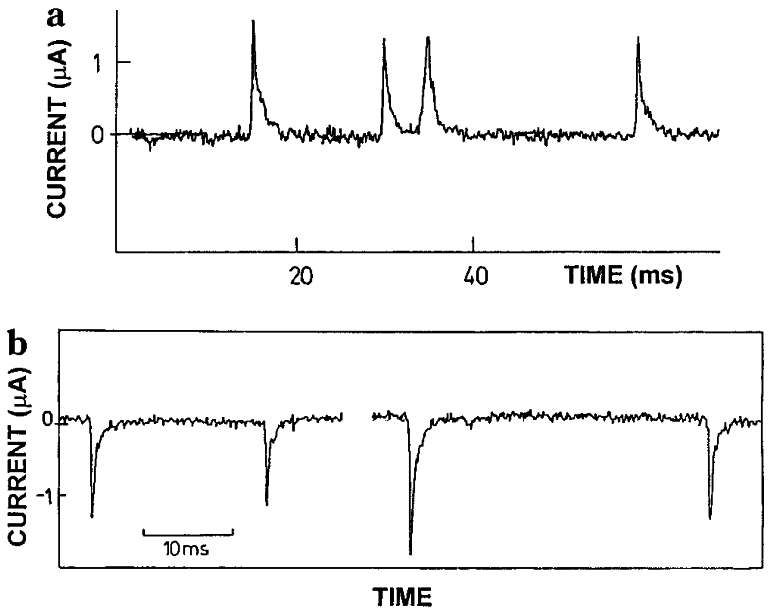

Figure 6. Current-time curve at the positively charged electrode (E = –400 mV, σ_{Hg} = +3.8 μC/cm^2) (a), and segments of current-time curves at the negatively charged electrode (E = -800 mV, σ_{Hg} = -6.5 μC/cm^2), (b), recorded in a deairated cell suspension of 5.4 × 10^5 cell/mL in 0.M NaCl. Adhesion signals appear as spikes superimposed on a flat background current. (Reprinted with permission from Svetličić, V., Ivošević, N., Kovač, S. and Žutić, V. 2000, Langmuir, 16, 8217. Copyright (2000) American Chemical Society).

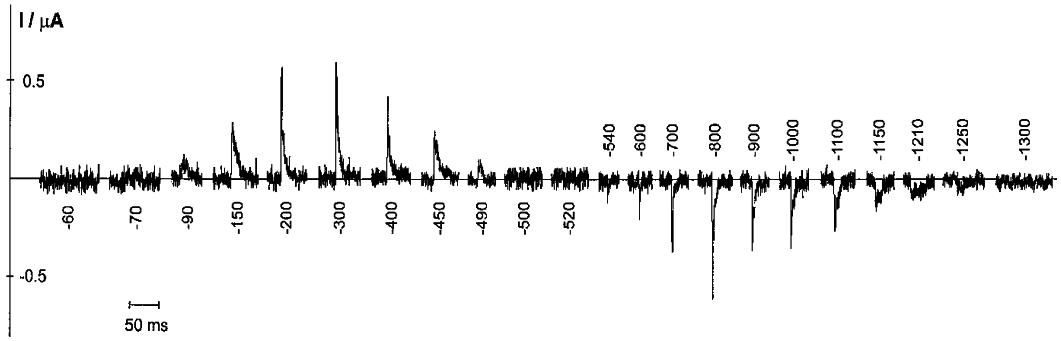

Figure 7. Adhesion signals of *D. tertiolecta* cells recorded in the whole potential range of appearance in 0.1 M NaCl electrolyte solution. The cell suspensions containing 2 x 10^4 cells/mL were deairated prior to measurement. Numbers next to the signals denote potentials in mV. (Reprinted from Svetličić, V. and Hozić, A. 2002, Electrophoresis, 23, 2080, with permission from John Wiley and Sons).

of displacement current. Subsequent signals on the same *i-t* curve do not seem to influence one another. The signals differ only slightly in the peak current and duration, indicating attachments from a nearly monodisperse particle population. The process is stochastic in nature and can be described by the Poisson distribution [21].

At *E*pzc, there is a potential region without net flow of displacement current; the adhesion signals are absent. The most positive edge of this region is defined as the potential of surface charge compensation, where charge density of the electrode equals the surface charge density of cell, E_C = –0.63 mC/cm^2. This was the first experimental determination of the surface charge density of a living marine phytoplankton cell [23]. There is clear evidence of cell rupture in the potential range of maximum attractive interaction, around *E*pzc [19], as the contact interface area, Ac, exceeds the cross-section area of a free cell by 2 orders of magnitude.

A great similarity to adhesion signals of droplets of liquid hydrocarbons [17] suggests that collective properties of cell exterior, rather than chemical composition, govern the dynamics of adhesion and rate of spreading, with fluidity playing a major role, The overall cell surface properties: fluidity, hydrophobicity and surface charge are manifested in the dynamics of individual adhesion events, which also reflect the physiological state [26-28] and the age of a single cell [25] (Figure 8).

The ranges of potentials of adhesion (Figure 7) are cell species specific [26]. These findings are in line with the AFM measurements of nanomechanical properties of living cells which, however, required a demanding experimental procedure [25, 53].

4. Adhesion signals of liposomes

Analogous to the adhesion-based studies of oil droplets and living cells [10-23] Scholz and coworkers characterized the adhesion of single liposomes from suspension onto static mercury drop electrode with an impressive progress made in the time-resolved data acquisition of the stochastic amperometric signals [29-34]. Specifically, the kinetic model for liposome adhesion on a mercury electrode [30] was constructed by analogy to the mechanistic events in fusion between curved lipid bilayers of two vesicles [54] with an eight-step mechanism of liposome adhesion at the mercury electrode (Figure 9) described by a system of six differential equations, further reduced to only three by pairwise addition. The truncated empirical equation of the three-step process was used to extract the kinetic parameters of the adhesion process by fitting the charge transient with five parameters. The first step of the liposome docking at the electrode (only a few lecithin molecules with the hydrophobic tails pointing outward of the bilayer are anchoring the liposome to the mercury surface) [30] was considered too fast to be resolved and recorded. The other two steps represent liposome opening and spreading.

The effects of liposome lamellarity, phase composition, size, curvature, and embedded molecules on the determination of time constants

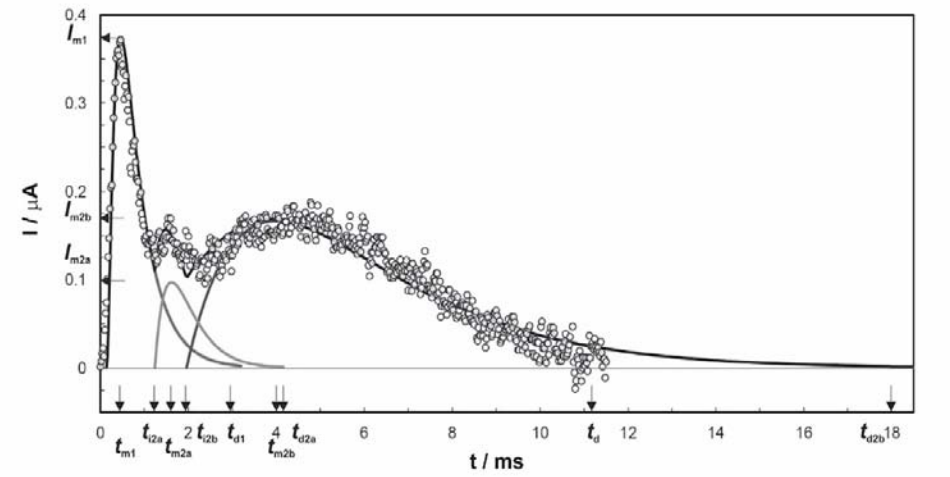

Figure 8. Amperometric signal of *D. tertiolecta* cell (circles) in the exponential phase of growth, recorded at a potential of −400 mV fitted with the reconstructed current transients obtained from the reaction kinetics model [25] and two exponential functions of time. (Reprinted with permission from Pillet, F., Dague, E., Pečar-Ilić, J., Ružić, I., Rols, M-P. and Ivošević DeNardis, N. 2019, Bioelectrochemistry, 127, 154. Copyright (2019) Elsevier).

and the activation energies of the processes were studied [31]. The mechanism of liposome adhesion was further investigated using high resolution chronoamperometric measurement to elucidate the initial stage of liposome interaction with the electrode. It was reported that the mechanisms of liposome adhesion and metal nucleation at the electrode share a similar stochastic nature and temporal distributions of the adhesion and nucleation events [34].

Understanding of the proposed mechanisms [30-32 and 34] was further discussed [18, 36, 55-57]. The claimed equivalence between molecular processes in the fusion of two vesicles and a liposome adhesion at the metallic surface (Figure 9) is inconsistent with the theory and the experimental evidence on liposome deformability, as well as with the orientation of polar groups of bilayer membranes in the process of liposome adhesion on hydrophilic and hydrophobic surfaces [18, 55 and references therein].

The molecular dynamic simulation study [18] examined the interactions of alkanes and phospholipids at charged interfaces and the results are consistent with interactions of phospholipid polar head groups with neutral mercury and gold electrodes. Previously reported electrochemical results [37, 55] confirm these findings by demonstrating bidirectional displacement currents

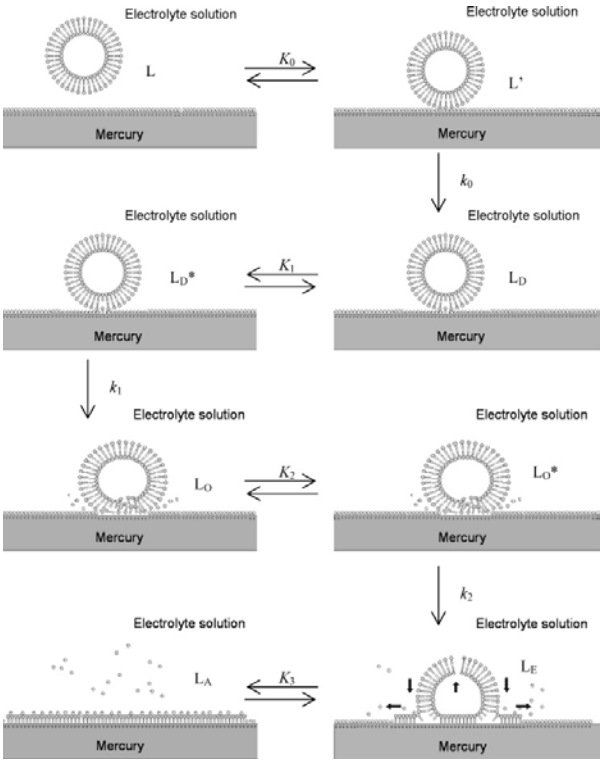

Figure 9. Proposed model of the adhesion process in the case of unilamellar liposomes (Reprinted with permission from Hellberg, D., Scholz, F., Schubert., F, Lovrić, M, Omanović, D., Agmo Hernández, V. and Thede, R. 2005, J. Phys.Chem. B, 109, 14715. Copyright (2005) American Chemical Society).

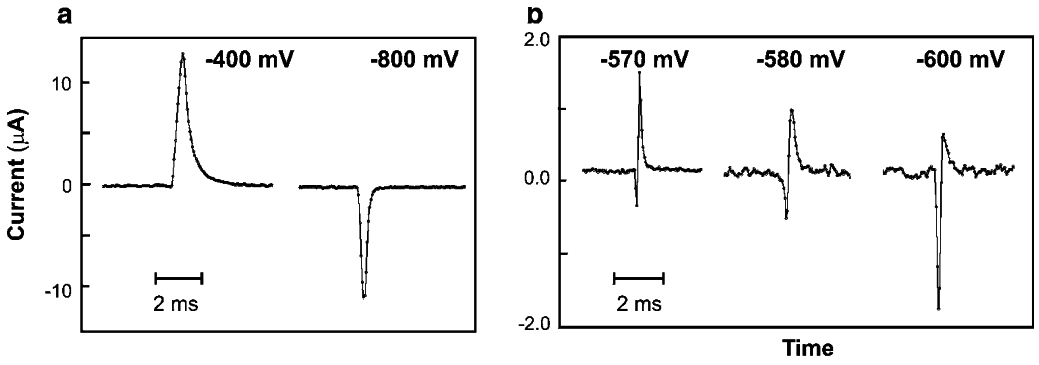

Figure 10. Adhesion signals of unilamelar DOPC liposomes in PBS. (a) unidirectional signals at positively, +3.3 μC/cm^2, and negatively charged electrode, −7.1 μC/cm^2; (b) bidirectional signals at moderately negatively charged electrode: -1.8 μC/cm^2, -2.1 μC/cm^2 and -2.6 μC/cm^2.

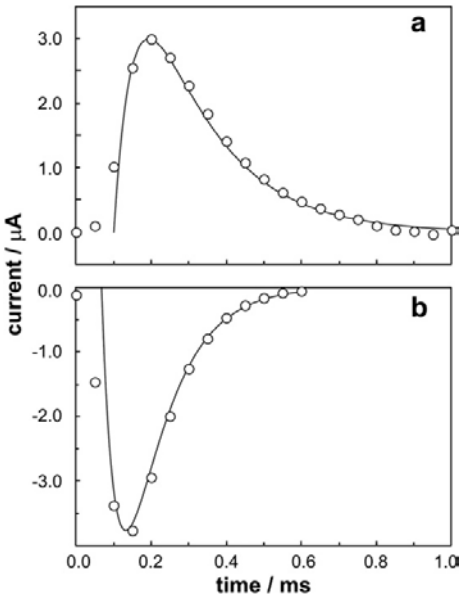

Figure 11. Amperometric signals (circles) recorded at potentials of −300 mV (a) and −800 mV (b) and corresponding reconstructed current transients (solid lines) obtained from the reaction kinetics model of the two-step process. (Reprinted with permission from Ivošević DeNardis, N., Ružić, I., Pečar-Ilić, J., El Shawish, S. and Ziherl, P. 2012, Bioelectrochem., 88, 48. Copyright (2012) Elsevier).

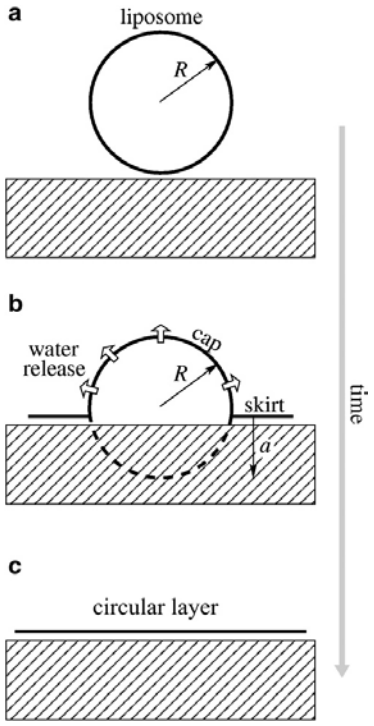

Figure 12. Three states of liposome adhesion at electrode surface (shaded area) according to a simplified mechanical model: the initial state of a spherical liposome (a), the intermediate state consisting of a spherical cap and a flat annular skirt adhering to the electrode (b), the final state of the circular layer (c).#In this simple geometry, the radius of the cap remains constant throughout the adhesion event. (Reprinted with permission from Ivošević DeNardis, N., Ružić, I., Pečar-Ilić, J., El Shawish, S. and Ziherl, P. 2012, Bioelectrochem., 88, 48. Copyright (2012) Elsevier)

from phospholipid vesicles adhering to moderately negatively charged interfaces (Figure 10), originating from the choline interactions observed in simulation.

Independently from the Scholz group, Ružić and coworkers [35, 36] developed a mathematical model for the kinetics of the adhesion event, based

on consecutive two- and three-step processes of the first-order to interpret the dynamics of liposome adhesion at the dropping mercury electrode:–the continuous transformation of the initial intact state to the intermediate deformed state and then to the final state of the lipid monolayer at the electrode. The three states were retrieved from amperometric signals (Figure 11), by combining predictions of the reaction kinetics model and a mechanical model based on the forces generated by the adhesion and the hydraulic resistance of the membrane.

The mechanical model advances the understanding of the physics of the adhesion event and offers interpretation of the three states identified by the reaction kinetics model (Figure 12). In particular, it suggests that the intermediate state consists of a spherical cap containing the remaining unreleased content of the liposome and a flat annular skirt closely bound to the electrode (Figure 12b). The liposome content is then released through transient pores formed in the cap membrane.

5. Conclusions

The re-emerged interest in traditional electroanalysis, amperometry at mercury drop electrodes, induced by discovery of stochastic adhesion signals of single microparticles at the dropping mercury electrode, preceded the more recent developments in the single entity electrochemistry SEE [3 and references therein]. The mercury electrode surface is atomically smooth, fluid, chemically inert, with well-known surface charge densities and interfacial tensions in a number of electrolyte solutions. By potentiostatic control of surface charge and tension at the aqueous electrolyte interface the adhesion forces can be fine-tuned. In such a way the interplay between electrostatic and hydrophobic interactions involved in individual soft particle adhesion can be sorted out. The reported research outlines the basic concepts for further development of SEE towards electrochemisrty of single soft particles, biological cells [58] and vesicles, which do not possess Faradaic activity, but the ability to produce capacitive signals upon attachment to electrodes.

The random occurrence of adhesion events is present as a more general phenomenon in the electroanalysis of dispersed systems [59], due to the spatial heterogeneity inherent to a dispersed system and to the stochastic nature of the particles' encounter with the electrode. Random processes are equally relevant in the case of submicron entities [60, 61 and references therein] and mercury ultramicroelectrodes [62].

Amperometric adhesion signals of individual living cells and vesicles contain unique information on the surface structure and charge density measured directly in the aqueous environment where their intrinsic properties are important for the biological activity. These results may well be useful in related biological studies involving cell adhesion, cell activity and cell fusion.

The extensive experimental research and modelling of amperometric adhesion signals of single liposomes included some contradicting interpretations of the mechanism and kinetics of adhesion. Further research is clearly needed to critically elucidate the stochastic adhesion signals at the molecular level.

Combining the fast and direct particle characterization through their adhesion signals with the high-resolution imaging by AFM sets the observation window below the micrometer scale that would allow direct characterization of submicron particle dynamics in marine environments by decoupling biotic production [63] from abiotic self-assembly processes of biopolymers in their formation [45, 46].

A technical pilot experiment demonstrated a possibility to continuously record the stochastic adhesion signals directly in the sea with DME immersed in seawater, the electrolyte, while the charge displacement signals are simultaneously amplified by the Faradaic charge transfer process of dissolved oxygen reduction.

ACKNOWLEDGEMENT

I thank many colleges who, over the years, made this work possible. I am grateful to Vesna Svetličić from the Rudjer Bošković Institue for the final comments, and to Sergey Prokhorov from the Samara National University for a correspondence on stochastic processes.

ABBREVIATIONS

AFM	:	atomic force microscopy
DME	:	dropping mercury electrode
DOPS	:	1,2-Dioleoyl-sn-glycero-3-phosphocholine

PBS : Phosphate-buffered saline
SEE : single entity electrochemstry

CONFLICT OF INTEREST STATEMENT

There are no conflicts of interest.

REFERENCES

1. Zvonarić, T., Žutić, V. and Branica, M. 1973, Thalassia Jugosl., 9, 736.
2. Zvonarić, T. 1975, Electrochemical Determination of Surface-Active Substances in Seawater, M.Sc. Thesis, Zagreb.
3. Baker, L. A. 2018, Am. Chem. Soc., 140, 15549.
4. Heyrovsky, J. and Kuta, J. 1965, Principles of Polarography, Czech. Acad, of Sci, Prague, eBook, 2013, Elsvier Science.
5. Bard, A. J. and Faulkner, L. R. 2001, Electrochemical Methods: Fundamentals and Applications, Wiley, New York, 2nd ed.
6. Frumkin, A. N., Fedorovich, B. B., Damaskin, E. V. and Krylov, J. 1974, J. Electroanal. Chem., 50, 103.
7. Marangoni, C. 1871, Ann. Phys. Chem. (Poggendorf), 143, 337.
8. Levich, V. G. 1962, Physicochemical Hydrodynamics, Prentice-Hall, Englewood Cliffs.
9. Sörensen, T. S. 1978, Dynamics and Instability of Fluid Interfaces, Lecture Notes on Physics 26, Springer Verlag, Berlin.
10. Pleše, T. and Žutić, V. 1984, J. Electroanal. Chem., 175, 299.
11. Žutić, V., Pleše, T., Tomaić, J. and Legović, T. 1984, Mol. Cryst. Liq. Cryst., 113,131.
12. Tomaić, J., Legović, T. and Žutić, V. 1989, J. Electroanal. Chem., 259, 49.
13. Žutić, V., Kovač, S., Tomaić, J. and Svetličić, V. 1993, J. Electroanal. Chem. 349, 173.
14. Ivošević, N., Tomaić, J. and Žutić, V. 1994, Langmuir, 10, 2415.
15. Ivošević, N. and Žutić, V. 1998, Langmuir 14, 231.
16. Ivošević, N., Žutić, V. and Tomaić, J. 1999, Langmuir, 15, 7063.
17. Tsekov, R. Kovač, S. and Žutić, V. 1999, Langmuir, 15, 5649.
18. Levine, Z. A., Ivosević DeNardis, N. and Vennier, P. T. 2016, Langmir, 32, 36280.
19. Svetličić, V., Ivošević, N., Kovač, S. and Žutić, V. 2000, Langmuir, 16, 8217.
20. News-Analytical-Currents, 2000, Anal. Chem., 72, 720A.
21. Kovač, S., Kraus, R., Geček, S. and Žutić, V. 2000, Croat. Chem. Acta, 73, 279.
22. Svetličić, V., Ivošević, N., Kovač, S. and Žutić, V. 2001, Biochem. Bioeng., 53, 79.
23. Svetličić, V. and Hozić, A. 2002, Electrophoresis, 23, 2080.
24. Ivošević DeNardis, N., Pečar-Ilić, J., Ružić, I. and Pletikapić, G. 2015, Electrochim. Acta, 176, 743.
25. Pillet, F., Dague, E., Pečar-Ilić, J., Ružić, I., Rols, M-P. and Ivošević DeNardis, N. 2019, Bioelectrochemistry, 127, 154.
26. Novosel, N. and Ivošević DeNardis, N. 2021, Electroanalysis, 33, 1.
27. Novosel, N., Mišić Radić, T., Zemla, J., Lekka, M., Čačković, A., Kasum, D,, Legović, T., Žutinić, P., Gligora Udovič, M. and Ivošević DeNardis, N. 2022, J. Appl. Phycol., 34, 243.
28. Novosel, N., Mišić Radić, T., Levak Zorinić, M., Zemla, J., Lekka M., Vrana, I., Gasparović, B., Horvat, L., Kasum, D. and Legović T., 2022, J. Appl. Phycol., 34, 1293.
29. Hellberg D., Scholz F., Schauer F. and Weitschies W. 2002, Electrochem. Commun, 4, 305.
30. Hellberg, D., Scholz, F., Schubert., F, Lovrić, M, Omanović, D., Agmo Hernández, V. and Thede, R. 2005, J. Phys.Chem. B, 109, 14715.
31. Agmo Hernández, V. and Scholz F. 2006, Langmuir, 22, 10723.
32. Agmo Hernández, V. and Scholz, F. 2008, Bioelectrochemistry, 74, 149.
33. Agmo Hernández, V., Hermes, M., Milchev, A.and Scholz, F. 2009, J. Solid State Electrochem., 13, 639.
34. Agmo Hernández, V., Milchev A., Scholz F. J. 2009, J. Solid State Electrochem., 13, 1111.
35. Ružić, I., Ivošević DeNardis, N. and Pečar-Ilić, J. 2009, Int. J. Electrochem.Sci., 4, 787.
36. Ivošević DeNardis, N., Ružić, I., Pečar-Ilić, J., El Shawish, S. and Ziherl, P. 2012, Bioelectrochem., 88, 48.

37. Ivošević DeNardis, N., Žutić, V., Svetličić, V. and Frkanec, R. 2012, Membr. Biol., 245, 573.
38. Žutić, V. and Legović, T. 1987, Nature, 328, 612.
39. Mantoura, R. F. C. 1987, Nature, 328, 579.
40. Marty, J.-C., Žutić, V., Precali, R., Saliot, A., Ćosović, B., Smodlaka, N. and Cauwet, G. 1988, Mar. Chem., 25, 243.
41. Žutić, V., Svetličić, V., Ivošević, N., Hozić, A. and Pečar, O. 2003, Period. Biol., 106, 67.
42. Svetličić, V., Žutić, V. and Tomaić, J. 1991, Mar. Chem., 32, 253.
43. Svetličić, V., Žutić, V. and Hozić Zimmermann, A. 2005, NY Acad.Sci., 1048, 524.
44. Kraus, R. and Ivošević DeNardis, N. 2023, Water, 15, 1665.
45. Žutić, V. and Svetličić, V. Interfacial Processes, 2000, The Handbook of Environmental Chemistry, Wangersky, P. (Ed.), Springer Verlag, Berlin.
46. Pletikapić, G., Svetličić, V., Lannon, H. U., Murvai, M. Kellermayer, M. and Brujić, J. 2014, Biophys. J., 107, 355.
47. Conway, B. E. 1969, Electrocchemical data, Greenwood Press, Westport.
48. Cox, D. R. 1955, Royal Stat. Soc. B, 17, 129.
49. Walk, C. Hand-book on Statistical Distributions for Experimentalists, 2007, University of Stockholm, Stockhom.
50. Adamson, W. A. and Gast, A. P. 1997, Wiley-Interscience, New York. Physical Chemistry of Surfaces, Wiley-Interscience, New York.
51. Israelachvili, J., Intermolecular and Surface Forces, 2011, Academic Press, San Diego, 3rd Ed.
52. Bongrand, P. 1988, Physical Basis of Cell-Cell Adhesion, CRC Press, Boca Raton.
53. Mišić Radić, T., Vukosav, P., Čačkovć, A. and Dulebo, A. 2023, Water, 15, 1983.
54. Lee, J. and Lentz, B. R. 1998, Proc. Natl. Acad. Sci. USA, 95, 9274.
55. Žutić, V. , Svetličić, V., Hozić Zimmermann, A., Ivošević DeNardis, N. and Frkanec, R. 2007, Langmuir, 23, 8647.
56. Hernandez, V. A. and Scholz, F. 2007, Langmuir, 23, 8650.
57. Scholz, F. J. 2011, Solid State Electrochem., 15, 169.
58. Zhang, J., Zhou, J., Pan, R., Jiang, D., Burgess, J. and Chen, H.-Y. 2018, ACS Sensors, 3, 242.
59. Žutić, V., Svetličić, V. and Tomaić, J. 1990, Pure & Appl. Chem., 62, 2269.
60. Boika, A. Thorgaard, S. N. and Bard, A. J. 2013, J. Phys. Chem. B, 117, 4371.
61. Zhang, J., He, S., Fang, T., Zhipeng, X., Sun, X., Yu, J., Ouyang, G., Huang, X. and Deng, H. J. 2023, Phys. Chem. B, 127, 8974.
62. Deng, Z., Elattar, R., Maroun, F. and Renault, C. 2018, Anal. Chem., 90, 12923.
63. Biller, S. J., Schubotz, F., Roggensack, S., Thompson, A. W., Summons, R. F. and Chrisholm, S. W. 2014, Science, 343, 183.